

Small- x behavior of the structure function F_2 and its slope $\partial \ln F_2 / \partial \ln(1/x)$ for “frozen” and analytic strong-coupling constants

G. Cvetič¹, A. Yu. Illarionov², B. A. Kniehl³, A. V. Kotikov^{3*}

¹ Department of Physics, Universidad Técnica Federico Santa María,
Avenida España 1680, Casilla 110–V, Valparaíso, Chile

² International School for Advanced Studies SISSA,
via Beirut 2–4, 34014 Trieste, Italy

³ II. Institut für Theoretische Physik, Universität Hamburg,
Luruper Chaussee 149, 22761 Hamburg, Germany

Abstract

Using the leading-twist approximation of the Wilson operator product expansion with “frozen” and analytic versions of the strong-coupling constant, we show that the Bessel-inspired behavior of the structure function F_2 and its slope $\partial \ln F_2 / \partial \ln(1/x)$ at small values of x , obtained for a flat initial condition in the DGLAP evolution equations, leads to good agreement with experimental data of deep-inelastic scattering at DESY HERA.

PACS: 12.38.Bx, 13.60.Hb

Keywords: Deep-inelastic scattering, Proton structure function

*On leave of absence from Bogoliubov Laboratory of Theoretical Physics, Joint Institute for Nuclear Research, 141980 Dubna, Moscow region, Russia.

1 Introduction

The experimental data from DESY HERA on the structure function F_2 of deep-inelastic scattering (DIS) [1,2,3,4,5,6,7,8,9,10,11,12,13,14] and its derivatives $\partial F_2/\partial \ln Q^2$ [4,6,15] and $\partial \ln F_2/\partial \ln(1/x)$ [15,16,17,18] bring us into a very interesting kinematic range for testing theoretical ideas on the behavior of quarks and gluons carrying a very small fraction of the proton's momentum, the so-called small- x region. In this limit, one expects that the conventional treatment based on the Dokshitzer-Gribov-Lipatov-Altarelli-Parisi (DGLAP) equations [19,20,21,22] does not account for contributions to the cross section which are leading in $\alpha_s \ln(1/x)$; moreover, the parton density functions (PDFs), in particular the one of the gluon, become large, and the need arises to apply a high-density formulation of QCD.

However, reasonable agreement between HERA data and the next-to-leading-order (NLO) approximation of perturbative QCD has been observed for $Q^2 \gtrsim 2 \text{ GeV}^2$ (see reviews in Ref. [23,24] and references cited therein) indicating that perturbative QCD can describe the evolution of F_2 and its derivatives down to very small Q^2 values, traditionally characterized by soft processes.

The standard program to study the x dependence of quark and gluon PDFs is to compare the numerical solutions of the DGLAP equations with the data and so to fit the parameters of the x profiles of the PDFs at some initial factorization scale Q_0^2 and the asymptotic scale parameter Λ . However, for analyzing exclusively the small- x region, there is the alternative of doing a simpler analysis by using some of the existing analytical solutions of the DGLAP equations in the small- x limit [25,26,27,28]. This was done in Ref. [25], where it was pointed out that the small- x data from HERA can be interpreted in terms of the so-called double-asymptotic-scaling (DAS) phenomenon related to the asymptotic behavior of the DGLAP evolution discovered in Ref. [29] many years ago.

The study of Ref. [25] was extended in Refs. [26,27,28] to include the subasymptotic part of the Q^2 evolution. This led to predictions [27,28] of the small- x asymptotic PDF forms in the framework of DGLAP dynamics starting at some initial value Q_0^2 with flat x distributions:

$$x f_a(x, Q_0^2) = A_a \quad (a = q, g), \quad (1)$$

where $f_a(x, Q^2)$ are the PDFs and A_a are unknown constants to be determined from the data. We refer to the approach of Refs. [26,27,28] as *generalized* DAS approximation. In this approach, the flat initial conditions in Eq. (1) play the basic role of the singular parts of the anomalous dimensions by determining the small- x asymptotics, as in the standard DAS case, while the contributions from the finite parts of the anomalous dimensions and from the Wilson coefficients can be considered as subasymptotic corrections, which are, however, important for better agreement with the experimental data. In the present paper, similarly to Refs. [25,26,27,28], we neglect the contribution from the non-singlet quark component.

The use of the flat initial condition given in Eq. (1) is supported by the actual experimental

situation: small- Q^2 data [4,6,11,15,30,31,32] are well described for $Q^2 \leq 0.4$ GeV² by Regge theory with Pomeron intercept $\alpha_P(0) = 1 + \lambda_P = 1.08$ (see Ref. [33] and references cited therein), close to the standard one, $\alpha_P(0) = 1$. The small rise of the HERA data [4,6,11,13,15] at small values of Q^2 can be explained, for instance, by contributions of higher-twist operators [28].

The purpose of this Letter is to compare the predictions for the structure function $F_2(x, Q^2)$ and its slope $\partial \ln F_2 / \partial \ln(1/x)$ from the generalized DAS approach with H1 and ZEUS experimental data [1,2,3,4,5,6,7,8,9,10,11,12,13,14,15,16,17,18]. Detailed inspection of the H1 data points [4,6,16] reveals that, in the ranges $x < 0.01$ and $Q^2 \gtrsim 2$ GeV², they exhibit a power-like behaviour of the form

$$F_2(x, Q^2) = Cx^{-\lambda(Q^2)}, \quad (2)$$

where the slope $\lambda(Q^2)$ is, to good approximation, independent of x and scales logarithmically with Q^2 , as $\lambda(Q^2) = a \ln(Q^2/\Lambda^2)$. A fit yields $C \approx 0.18$, $a \approx 0.048$, and $\Lambda = 292$ MeV [16]. The linear rise of $\lambda(Q^2)$ with $\ln Q^2$ is also indicated in Figs. 2 and 3, to be discussed below.

The rise of $\lambda(Q^2)$ linearly with $\ln Q^2$ can be traced to strong nonperturbative physics (see Ref. [34] and references cited therein), i.e. $\lambda(Q^2) \sim 1/\alpha_s(Q^2)$. However, the analysis of Ref. [35] demonstrated that this rise can be explained naturally in the framework of perturbative QCD (see also Section 3).

The H1 and ZEUS Collaborations [15,17,18] also presented new data for $\lambda(Q^2)$ at quite small values of Q^2 . As may be seen from Fig. 8 of Ref. [15], the ZEUS value for $\lambda(Q^2)$ is consistent with a constant of about 0.1 at $Q^2 \lesssim 0.6$ GeV², as is expected under the assumption of single-soft-Pomeron exchange within the framework of Regge phenomenology.

It is interesting to extend the analysis of Ref. [35] to the small- Q^2 range with the help of the well-known infrared modifications of the strong-coupling constant. We shall adopt the ‘‘frozen’’ [36] and analytic [37] versions.

This paper is organized as follows. Section 2 contains basic formulae for the structure function F_2 and its slope $\partial \ln F_2 / \partial \ln(1/x)$ in the generalized DAS approximation [27,28,35], which are needed for the present study. In Section 3, we compare our results on F_2 and $\partial \ln F_2 / \partial \ln(1/x)$ with experimental data. Our conclusions may be found in Section 4.

2 Generalized DAS approach

The flat initial conditions in Eq. (1) correspond to the case when the PDFs tend to constants as $x \rightarrow 0$ at some initial value Q_0^2 . The main ingredients of the results at the

leading order (LO) [27,28] include the following.¹ Both, the gluon and quark-singlet PDFs are presented in terms of two components (“+” and “-”),

$$F_2(x, Q^2) = e x f_q(x, Q^2), \quad f_a(x, Q^2) = f_a^+(x, Q^2) + f_a^-(x, Q^2) \quad (a = q, g), \quad (3)$$

which are obtained from the analytic Q^2 -dependent expressions of the corresponding (“+” and “-”) PDF moments. Here, $e = (\sum_{i=1}^f e_i^2)/f$ is the average charge square and f is the number of active quark flavors. The small- x asymptotic results for the PDFs f_a^\pm are

$$\begin{aligned} x f_q^+(x, Q^2) &= \frac{f}{9} \left(A_g + \frac{4}{9} A_q \right) \rho \tilde{I}_1(\sigma) e^{-\bar{d}_+(1)s} + O(\rho), & f_g^+(x, Q^2) &= \frac{9 \tilde{I}_0(\sigma)}{f \rho \tilde{I}_1(\sigma)} f_q^+(x, Q^2), \\ x f_q^-(x, Q^2) &= A_q e^{-d_-(1)s} + O(x), & f_g^-(x, Q^2) &= -\frac{4}{9} f_q^-(x, Q^2), \end{aligned} \quad (4)$$

where $\bar{d}_+(1) = 1 + 20f/(27\beta_0)$ and $d_-(1) = 16f/(27\beta_0)$ are the regular parts of the anomalous dimensions $d_+(n)$ and $d_-(n)$, respectively, in the limit $n \rightarrow 1$.² Here, n is the variable in Mellin space. The functions \tilde{I}_ν ($\nu = 0, 1$) are related to the modified Bessel function I_ν and the Bessel function J_ν by

$$\tilde{I}_\nu(\sigma) = \begin{cases} I_\nu(\sigma), & \text{if } s \geq 0; \\ i^{-\nu} J_\nu(i\sigma), & \text{if } s < 0. \end{cases} \quad (5)$$

The variables s , σ , and ρ are given by

$$s = \ln \frac{\alpha_s^{\text{LO}}(Q_0^2)}{\alpha_s^{\text{LO}}(Q^2)}, \quad \sigma = 2\sqrt{\hat{d}_+(s - i\epsilon) \ln x}, \quad \rho = \frac{\sigma}{2 \ln(1/x)}, \quad (6)$$

where $\hat{d}_+ = -12/\beta_0$, $\alpha_s^{\text{LO}}(Q^2)$ is the strong-coupling constant in the LO approximation, and β_0 is the first term of its β function.

Contrary to the approach of Refs. [25,26,27,28], various groups were able to fit the available data using a hard input at small values of x , of the form $x^{-\lambda}$, with different values $\lambda > 0$ at small and large values of Q^2 [33,38,39,40,41,42,43,44,45,46,47,48]. At small Q^2 values, there are well-known such results [33]. At large Q^2 values, this is not very surprising for the modern HERA data because they cannot distinguish between the behavior based on a steep PDF input at quite large Q^2 values and the steep form acquired after the dynamical evolution from a flat initial condition at quite small Q^2 values.

As has been shown in Refs. [27,28], the x dependencies of F_2 and the PDFs given by the Bessel-like forms in the generalized DAS approach can mimic power-law shapes over a limited region of x and Q^2 values:

$$F_2(x, Q^2) \sim x^{-\lambda_{F_2}^{\text{eff}}(x, Q^2)}, \quad x f_a(x, Q^2) \sim x^{-\lambda_a^{\text{eff}}(x, Q^2)}. \quad (7)$$

¹ The NLO results may be found in Refs. [27,28].

²We denote the singular and regular parts of a given quantity $k(n)$ in the limit $n \rightarrow 1$ by $\hat{k}(n)$ and $\bar{k}(n)$, respectively.

In the twist-two LO approximation, the effective slopes have the following forms:

$$\lambda_{F_2}^{\text{eff}}(x, Q^2) = \lambda_q^{\text{eff}}(x, Q^2) = \frac{f_q^+(x, Q^2)}{f_q(x, Q^2)} \rho \frac{\tilde{I}_2(\sigma)}{\tilde{I}_1(\sigma)}, \quad \lambda_g^{\text{eff}}(x, Q^2) = \frac{f_g^+(x, Q^2)}{f_g(x, Q^2)} \rho \frac{\tilde{I}_1(\sigma)}{\tilde{I}_0(\sigma)}. \quad (8)$$

The corresponding NLO expressions and the higher-twist terms may be found in Refs. [27,28].

The effective slopes $\lambda_{F_2}^{\text{eff}}$ and λ_a^{eff} depend on the magnitudes A_a of the initial PDFs and also on the chosen input values of Q_0^2 and Λ . To compare with the experimental data, it is necessary to use the exact expressions from Eq. (8), but for a qualitative analysis one can use some appropriate approximations. At large values of Q^2 , the “-” components of the PDFs are negligible, and the dependencies of the slopes on the PDFs disappear. In this case, the asymptotic behaviors of the slopes are given by the following expressions:³

$$\lambda_q^{\text{eff,as}}(x, Q^2) \approx \rho - \frac{3}{4 \ln(1/x)}, \quad \lambda_g^{\text{eff,as}}(x, Q^2) \approx \rho - \frac{1}{4 \ln(1/x)}. \quad (9)$$

where the symbol \approx marks the approximation obtained from the expansion of the usual and modified Bessel functions in Eq. (5). One can see from Eq. (9) that the gluon effective slope $\lambda_g^{\text{eff,as}}$ is larger than the quark one $\lambda_q^{\text{eff,as}}$, which is in excellent agreement with global analyses [23,24].

3 Comparison with experimental data

Using the results of the previous sections, we analyze HERA data for the structure function F_2 and its slope $\partial \ln F_2 / \partial \ln(1/x)$ at small x values from the H1 and ZEUS Collaborations [1,2,3,4,5,6,7,8,9,10,11,12,13,14,15,16,17,18]. The experimental results for the x dependence of F_2 in bins of Q^2 are shown in Fig. 1, while the Q^2 dependence of $\lambda_{F_2}^{\text{eff}}(x, Q^2)$ for an average small- x value of 10^{-3} are shown in Figs. 2 and 3.

In order to keep the analysis as simple as possible, we fix $f = 4$ and $\alpha_s^{\overline{\text{MS}}}(M_Z^2) = 0.1166$, so that $\Lambda_{\overline{\text{MS}}}^{(4)} = 284$ MeV and $\Lambda_{\text{LO}}^{(4)} = 112$ MeV, in agreement with the more recent ZEUS results [14]. We fit the combined H1 and ZEUS data on F_2 [1,2,3,4,5,6,7,8,9,10,11,12,13,14] at LO and NLO imposing two different cuts on Q^2 , namely $Q^2 > 1.5$ GeV² and $Q^2 > 0.5$ GeV². The resulting values for A_g , A_q , and Q_0^2 are collected in Table 1 together with the values of χ^2 per data point ($\chi^2/\text{n.d.f.}$) achieved. In Fig. 1, the H1 and ZEUS data on F_2 , which come as x distributions in bins of Q^2 , are compared with the NLO result obtained with the cut $Q^2 > 0.5$ GeV². Furthermore, the Q^2 dependence of $\lambda_{F_2}^{\text{eff}}(x, Q^2)$ as determined by H1 and ZEUS at an average small- x value of 10^{-3} is confronted with the result of the NLO fit for $Q^2 > 0.5$ GeV² in Fig. 2.

³The asymptotic formulae given in Eq. (9) work quite well at any values $Q^2 \geq Q_0^2$, because at $Q^2 = Q_0^2$ the values of λ_a^{eff} and $\lambda_{F_2}^{\text{eff}}$ are equal to zero. The use of the approximations in Eq. (9) instead of the exact results given in Eq. (8) underestimates (overestimates) the gluon (quark) slope at $Q^2 \geq Q_0^2$ only slightly.

Table 1: Results of the LO and NLO fits to H1 and ZEUS data [1,2,3,4,5,6,7,8,9,10,11,12,13,14] for different small- Q^2 cuts.

	A_g	A_q	Q_0^2 [GeV 2]	$\chi^2/\text{n.d.f.}$
$Q^2 \geq 1.5$ GeV 2				
LO	0.784 ± 0.016	0.801 ± 0.019	0.304 ± 0.003	754/609
LO an.	0.932 ± 0.017	0.707 ± 0.020	0.339 ± 0.003	632/609
LO fr.	1.022 ± 0.018	0.650 ± 0.020	0.356 ± 0.003	547/609
NLO	-0.200 ± 0.011	0.903 ± 0.021	0.495 ± 0.006	798/609
NLO an.	0.310 ± 0.013	0.640 ± 0.022	0.702 ± 0.008	655/609
NLO fr.	0.180 ± 0.012	0.780 ± 0.022	0.661 ± 0.007	669/609
$Q^2 \geq 0.5$ GeV 2				
LO	0.641 ± 0.010	0.937 ± 0.012	0.295 ± 0.003	1090/662
LO an.	0.846 ± 0.010	0.771 ± 0.013	0.328 ± 0.003	803/662
LO fr.	1.127 ± 0.011	0.534 ± 0.015	0.358 ± 0.003	679/662
NLO	-0.192 ± 0.006	1.087 ± 0.012	0.478 ± 0.006	1229/662
NLO an.	0.281 ± 0.008	0.634 ± 0.016	0.680 ± 0.007	633/662
NLO fr.	0.205 ± 0.007	0.650 ± 0.016	0.589 ± 0.006	670/662

Because the twist-two approximation is only reasonable at $Q^2 \gtrsim 2.5$ GeV 2 [28], as may be seen from Fig. 1, some theoretical improvements are necessary for smaller Q^2 values. In Ref. [28], the higher-twist corrections through twist six were added to find good agreement for $Q^2 \gtrsim 0.5$ GeV 2 . However, the twist-four and twist-six terms increase the number of parameters, which become strongly correlated.

Here, we investigate an alternative possibility, namely to modify the strong-coupling constant in the infrared region. Specifically, we consider two modifications, which effectively increase the argument of the strong-coupling constant at small Q^2 values, in accordance with Refs. [49,50,51,52,53,54]. In the first case, which is more phenomenological, we introduce a freezing of the strong-coupling constant by changing its argument as $Q^2 \rightarrow Q^2 + M_\rho^2$, where M_ρ is the rho-meson mass [36]. Thus, in the formulae of Section 2 and their NLO generalizations [27,28], we introduce the following replacement

$$\alpha_s^i(Q^2) \rightarrow \alpha_{\text{fr}}^i(Q^2) = \alpha_s^i(Q^2 + M_\rho^2) \quad (i = \text{LO}, \overline{\text{MS}}), \quad (10)$$

where $\alpha_s^{\text{LO}}(Q^2)$ and $\alpha_s^{\overline{\text{MS}}}(Q^2)$ have the canonical forms dictated by the renormalization group.

The second possibility is based on the idea by Shirkov and Solovtsov [37,55] (see also the recent reviews in Refs. [56,57,58] and the references cited therein) regarding the analyticity of the strong-coupling constant that leads to an additional power dependence. In this case, the one-loop and two-loop coupling constants $\alpha_s^{\text{LO}}(Q^2)$ and $\alpha_s^{\overline{\text{MS}}}(Q^2)$ appearing in

the formulae of the previous sections and their NLO generalizations are to be replaced as

$$\begin{aligned}\alpha_s^{\text{LO}}(Q^2) &\rightarrow \alpha_{\text{an}}^{\text{LO}}(Q^2) = \alpha_s^{\text{LO}}(Q^2) - \frac{1}{\beta_0} \frac{\Lambda_{\text{LO}}^2}{Q^2 - \Lambda_{\text{LO}}^2}, \\ \alpha_s^{\overline{\text{MS}}}(Q^2) &\rightarrow \alpha_{\text{an}}^{\overline{\text{MS}}}(Q^2) = \alpha_s^{\overline{\text{MS}}}(Q^2) - \frac{1}{2\beta_0} \frac{\Lambda_{\overline{\text{MS}}}^2}{Q^2 - \Lambda_{\overline{\text{MS}}}^2} + \dots,\end{aligned}\tag{11}$$

where the ellipsis stands for cut terms which give negligible contributions.

We thus repeat the LO and NLO fits discussed above using in turn the frozen and analytic versions of the strong-coupling constant according to the replacements of Eqs. (10) and (11), respectively. The results for F_2 are included in Table 1 and Fig. 1 and those for $\lambda_{F_2}^{\text{eff}}(x, Q^2)$ in Fig. 2. Figure 1, as also Fig. 5 in Ref. [28], only covers the small- Q^2 region, $Q^2 < 9.22 \text{ GeV}^2$, because the three NLO predictions are hardly distinguishable at larger values of Q^2 .

From Fig. 1, we observe that the fits based on the frozen and analytic strong-coupling constants are very similar and describe the data in the small- Q^2 range significantly better than the canonical fit. This is also reflected in the values of $\chi^2/\text{n.d.f.}$ listed in Table 1. The improvement is especially striking at NLO if data with very small Q^2 values, with $Q^2 \geq 0.5 \text{ GeV}^2$, are included in the fits. Then $\chi^2/\text{n.d.f.}$ is almost reduced by a factor of two to assume values close to unity when the canonical version of the strong-coupling constant is replaced by the frozen or analytic ones. The situation is very similar to the case when the higher-twist corrections according to the renormalon model are included [28]. In order to illustrate this, we display in Fig. 1 also the results obtained at NLO in the renormalon model of higher-twist terms, which are taken from Fig. 5 in Ref. [28]. We see that the latter describe the experimental data slightly better for $0.65 \text{ GeV}^2 \lesssim Q^2 \lesssim 2.0 \text{ GeV}^2$ than the results obtained here, which is also reflected in the values of $\chi^2/\text{n.d.f.}$ achieved, namely $\chi^2/\text{n.d.f.} = 565/658 = 0.86$ for renormalon improvement versus $\chi^2/\text{n.d.f.} = 633/662 = 0.96$ and $670/662 = 1.01$ for analytic and frozen strong-coupling constants, respectively. However, one should bear in mind that this improvement happens at the expense of introducing four additional adjustable parameters.

Figure 2 nicely demonstrates that the theoretical description of the small- Q^2 ZEUS data on $\lambda_{F_2}^{\text{eff}}(x, Q^2)$ by NLO QCD is significantly improved by implementing the frozen and analytic strong-coupling constants. Again, these two alternatives lead to very similar results. For comparison, the linear rise of $\lambda_{F_2}^{\text{eff}}(x, Q^2)$ with $\ln Q^2$ as described by Eq. (2) is also indicated in Fig. 2. For comparison, we display in Fig. 2 also the results obtained by Kaidalov et al. [47] and by Donnachie and Landshoff [48] adopting phenomenological models based on Regge theory. While they yield an improved description of the experimental data for $Q^2 \lesssim 0.4 \text{ GeV}^2$, the agreement generally worsens in the range $2 \text{ GeV}^2 \lesssim Q^2 \lesssim 8 \text{ GeV}^2$.

As may be seen from Table 1, the three NLO fits for $F_2(x, Q^2)$ yield $Q_0^2 \approx 0.5\text{--}0.7 \text{ GeV}^2$ (see also Ref. [28]). Figure 2 shows that the conventional NLO fit yields $\lambda_{F_2}^{\text{eff}}(x, Q_0^2) = 0$ as suggested by Eq. (1). The replacements of Eqs. (10) and (11) raise the value of $\lambda_{F_2}^{\text{eff}}(x, Q_0^2)$. In fact, the results for $\lambda_{F_2}^{\text{eff}}(x, Q^2)$ obtained with the frozen and analytic versions of the

strong-coupling constant agree much better with the ZEUS data at $Q^2 \gtrsim 0.5 \text{ GeV}^2$. Nevertheless, for $Q^2 < 0.5 \text{ GeV}^2$, there is still some disagreement with the data, which needs additional investigation.

In Fig. 2, the NLO results for $\lambda_{F_2}^{\text{eff}}(x, Q^2)$ are evaluated at $x = 10^{-3}$. In Fig. 3, we study the variation with x in the range $10^{-5} < x < 10^{-2}$. For simplicity, we only do this for the case of the frozen strong-coupling constant; the result for the analytic one would be very similar. We observe good agreement between the experimental data and the generalized DAS approach for a broad range of small- x values. At small Q^2 values, $\lambda_{F_2}^{\text{eff}}(x, Q^2)$ is practically independent of x , which is because the variable ρ defined in Eq. (6) takes rather small values there. At large Q^2 values, the x dependence of $\lambda_{F_2}^{\text{eff}}(x, Q^2)$ is rather strong. However, it is well known that the boundaries and mean values of the experimental x ranges [16] increase proportionally with Q^2 , which is related to the kinematical restrictions in the HERA experiments, namely $x \sim 10^{-4} \times Q^2$ (see Refs. [4,6,13,14] and, for example, Fig. 1 of Ref. [15]). From Fig. 3, we see that the HERA data are close to $\lambda_{F_2}^{\text{eff}}(x, Q^2)$ at $x \sim 10^{-4}$ – 10^{-5} for $Q^2 = 4 \text{ GeV}^2$ and at $x \sim 10^{-2}$ for $Q^2 = 100 \text{ GeV}^2$. Indeed, the correlations between x and Q^2 of the form $x_{\text{eff}} = a \times 10^{-4} \times Q^2$ with $a = 0.1$ and 1 lead to a modification of the Q^2 evolution which starts to resemble $\ln Q^2$, rather than $\ln \ln Q^2$ as is standard [35].

4 Conclusions

We studied the Q^2 dependence of the structure function F_2 and the slope $\lambda_{F_2}^{\text{eff}} = \partial \ln F_2 / \partial \ln(1/x)$ at small x values in the framework of perturbative QCD. Our twist-two results are in very good agreement with HERA data [1,2,3,4,5,6,7,8,9,10,11,12,13,14,15,16,17,18] at $Q^2 \gtrsim 2.5 \text{ GeV}^2$, where perturbation theory is applicable. The applications of the frozen and analytic versions of the strong-coupling constants, $\alpha_{\text{fr}}^{\overline{\text{MS}}}(Q^2)$ and $\alpha_{\text{an}}^{\overline{\text{MS}}}(Q^2)$, significantly improve the agreement with the HERA data [1,2,3,4,5,6,7,8,9,10,11,12,13,14,15,16,17,18] for both the structure function F_2 and its slope $\lambda_{F_2}^{\text{eff}}(x, Q^2)$ for small Q^2 values, $Q^2 \gtrsim 0.5 \text{ GeV}^2$. The results obtained with these infrared-modified strong-coupling constants and also those based on the renormalon model with higher-twist terms incorporated, which were considered in Ref. [28], are very similar numerically.

As a next step of our investigations, we plan to fit the HERA data [1,2,3,4,5,6,7,8,9,10,11,12,13,14] for $F_2(x, Q^2)$ using alternative analytic versions of the strong-coupling constant (see, for example, the recent reviews in Refs. [56,57,58]), to find out if the theoretical description of the slope $\lambda_{F_2}^{\text{eff}}$ can be further improved at small Q^2 values.

Acknowledgments

The work of G.C. was supported in part by Chilean Fondecyt Grant No. 1095196. The work of B.A.K. was supported in part by the German Federal Ministry for Education and Research BMBF through Grant No. 05 HT6GUA and by the Helmholtz Association HGF through Grant No. HA 101. The work of A.V.K. was supported in part by the German Research Foundation DFG through Grant No. INST 152/465–1, by the Heiserberg-Landau Program through Grant No. 5, and by the Russian Foundation for Basic Research through Grant No. 08–02–00896–a.

References

- [1] I. Abt *et al.* (H1 Collaboration), Nucl. Phys. **B407**, 515 (1993).
- [2] T. Ahmed *et al.* (H1 Collaboration), Nucl. Phys. **B439**, 471 (1995), hep-ex/9503001.
- [3] S. Aid *et al.* (H1 Collaboration), Nucl. Phys. **B470**, 3 (1996), hep-ex/9603004.
- [4] C. Adloff *et al.* (H1 Collaboration), Nucl. Phys. **B497**, 3 (1997), hep-ex/9703012.
- [5] C. Adloff *et al.* (H1 Collaboration), Eur. Phys. J. **C13**, 609 (2000), hep-ex/9908059.
- [6] C. Adloff *et al.* (H1 Collaboration), Eur. Phys. J. **C21**, 33 (2001), hep-ex/0012053.
- [7] M. Derrick *et al.* (ZEUS Collaboration), Phys. Lett. **B316**, 412 (1993).
- [8] M. Derrick *et al.* (ZEUS Collaboration), Z. Phys. **C65**, 379 (1995).
- [9] M. Derrick *et al.* (ZEUS Collaboration), Z. Phys. **C69**, 607 (1996), hep-ex/9510009.
- [10] M. Derrick *et al.* (ZEUS Collaboration), Z. Phys. **C72**, 399 (1996), hep-ex/9607002.
- [11] J. Breitweg *et al.* (ZEUS Collaboration), Phys. Lett. **B407**, 432 (1997), hep-ex/9707025.
- [12] J. Breitweg *et al.* (ZEUS Collaboration), Eur. Phys. J. **C7**, 609 (1999), hep-ex/9809005.
- [13] J. Breitweg *et al.* (ZEUS Collaboration), Phys. Lett. **B487**, 53 (2000), hep-ex/0005018.
- [14] S. Chekanov *et al.* (ZEUS Collaboration), Eur. Phys. J. **C21**, 443 (2001), hep-ex/0105090.
- [15] B. Surrow (on behalf of the H1 and ZEUS Collaborations), in D. Horvath, P. Levai, and A. Patkos, eds., *Proceedings of International Europhysics Conference on High Energy Physics, Budapest, Hungary, 2001*, PoS(hep2001)052, hep-ph/0201025.

- [16] C. Adloff *et al.* (H1 Collaboration), Phys. Lett. **B520**, 183 (2001), hep-ex/0108035.
- [17] T. Lastovicka (on behalf of the H1 Collaboration), Acta Phys. Polon. **B33**, 2835 (2002).
- [18] J. Gayler (on behalf of the H1 Collaboration), Acta Phys. Polon. **B33**, 2841 (2002), hep-ex/0206062.
- [19] V. N. Gribov and L. N. Lipatov, Sov. J. Nucl. Phys. **15**, 438 (1972).
- [20] L. N. Lipatov, Sov. J. Nucl. Phys. **20**, 94 (1975).
- [21] G. Altarelli and G. Parisi, Nucl. Phys. **B126**, 298 (1977).
- [22] Y. L. Dokshitzer, Sov. Phys. JETP **46**, 641 (1977), [Zh. Eksp. Teor. Fiz. **73**, 1216 (1977)].
- [23] A. M. Cooper-Sarkar, R. C. E. Devenish, and A. De Roeck, Int. J. Mod. Phys. **A13**, 3385 (1998), hep-ph/9712301.
- [24] A. V. Kotikov, Phys. Part. Nucl. **38**, 1 (2007), [Erratum-ibid. **38** (2007) 828].
- [25] R. D. Ball and S. Forte, Phys. Lett. **B336**, 77 (1994), hep-ph/9406385.
- [26] L. Mankiewicz, A. Saalfeld, and T. Weigl, Phys. Lett. **B393**, 175 (1997), hep-ph/9612297.
- [27] A. V. Kotikov and G. Parente, Nucl. Phys. **B549**, 242 (1999), hep-ph/9807249.
- [28] A. Y. Illarionov, A. V. Kotikov, and G. Parente Bermudez, Phys. Part. Nucl. **39**, 307 (2008), hep-ph/0402173.
- [29] A. D. Rújula, S. L. Glashow, H. D. Politzer, S. B. Treiman, F. Wilczek, and A. Zee, Phys. Rev. **D10**, 1649 (1974).
- [30] M. Arneodo *et al.* (New Muon Collaboration), Phys. Lett. **B364**, 107 (1995), hep-ph/9509406.
- [31] M. Arneodo *et al.* (New Muon Collaboration), Nucl. Phys. **B483**, 3 (1997), hep-ph/9610231.
- [32] M. R. Adams *et al.* (E665 Collaboration), Phys. Rev. **D54**, 3006 (1996).
- [33] A. Donnachie and P. V. Landshoff, Phys. Lett. **B437**, 408 (1998), hep-ph/9806344.
- [34] F. Schrempp, *Instanton-induced processes: An overview* (2005), hep-ph/0507160.
- [35] A. V. Kotikov and G. Parente, J. Exp. Theor. Phys. **97**, 859 (2003), [Zh. Eksp. Teor. Fiz. **97**, 963 (2003)], hep-ph/0207276.

- [36] B. Badelek, J. Kwiecinski, and A. Stasto, *Z. Phys.* **C74**, 297 (1997), hep-ph/9603230.
- [37] D. V. Shirkov and I. L. Solovtsov, *Phys. Rev. Lett.* **79**, 1209 (1997), hep-ph/9704333.
- [38] H. Abramowicz, E. M. Levin, A. Levy, and U. Maor, *Phys. Lett.* **B269**, 465 (1991).
- [39] A. V. Kotikov, *Phys. Atom. Nucl.* **56**, 1276 (1993), [*Yad. Fiz.* **56**, 217 (1993)].
- [40] L. L. Jenkovszky, A. V. Kotikov, and F. Paccanoni, *Phys. Lett.* **B314**, 421 (1993).
- [41] A. Capella, A. Kaidalov, C. Merino, and J. Tran Thanh Van, *Phys. Lett.* **B337**, 358 (1994), hep-ph/9405338.
- [42] G. M. Frichter, D. W. McKay, and J. P. Ralston, *Phys. Rev. Lett.* **74**, 1508 (1995), [Erratum-*ibid.* **77**, 4107 (1996)], hep-ph/9409433.
- [43] A. V. Kotikov, *Mod. Phys. Lett.* **A11**, 103 (1996), hep-ph/9504357.
- [44] A. V. Kotikov, *Phys. Atom. Nucl.* **59**, 2137 (1996), [*Yad. Fiz.* **59**, 2219 (1996)].
- [45] C. López, F. Barreiro, and F. J. Ynduráin, *Z. Phys.* **C72**, 561 (1996).
- [46] K. Adel, F. Barreiro, and F. J. Ynduráin, *Nucl. Phys.* **B495**, 221 (1997), hep-ph/9610380.
- [47] A. B. Kaidalov, C. Merino, and D. Pertermann, *Eur. Phys. J.* **C20**, 301 (2001), hep-ph/0004237.
- [48] A. Donnachie and P. V. Landshoff, *Acta Phys. Polon.* **B34**, 2989 (2003), hep-ph/0305171.
- [49] A. V. Kotikov, *Phys. Lett.* **B338**, 349 (1994).
- [50] Y. L. Dokshitzer and D. V. Shirkov, *Z. Phys.* **C67**, 449 (1995).
- [51] S. J. Brodsky, V. S. Fadin, V. T. Kim, L. N. Lipatov, and G. B. Pivovarov, *JETP Lett.* **70**, 155 (1999), hep-ph/9901229.
- [52] M. Ciafaloni, D. Colferai, and G. P. Salam, *JHEP* **07**, 054 (2000), hep-ph/0007240.
- [53] G. Altarelli, R. D. Ball, and S. Forte, *Nucl. Phys.* **B621**, 359 (2002), hep-ph/0109178.
- [54] B. Andersson *et al.* (Small x Collaboration), *Eur. Phys. J.* **C25**, 77 (2002), hep-ph/0204115.
- [55] I. L. Solovtsov and D. V. Shirkov, *Theor. Math. Phys.* **120**, 1220 (1999), hep-ph/9909305.
- [56] A. P. Bakulev and S. V. Mikhailov, *Resummation in (F)APT* (2008), arXiv:0803.3013.

- [57] G. Cvetič and C. Valenzuela, *Braz. J. Phys.* **38**, 371 (2008), arXiv:0804.0872.
- [58] N. G. Stefanis, *Taming Landau singularities in QCD perturbation theory: The analytic approach* (2009), arXiv:0902.4805.

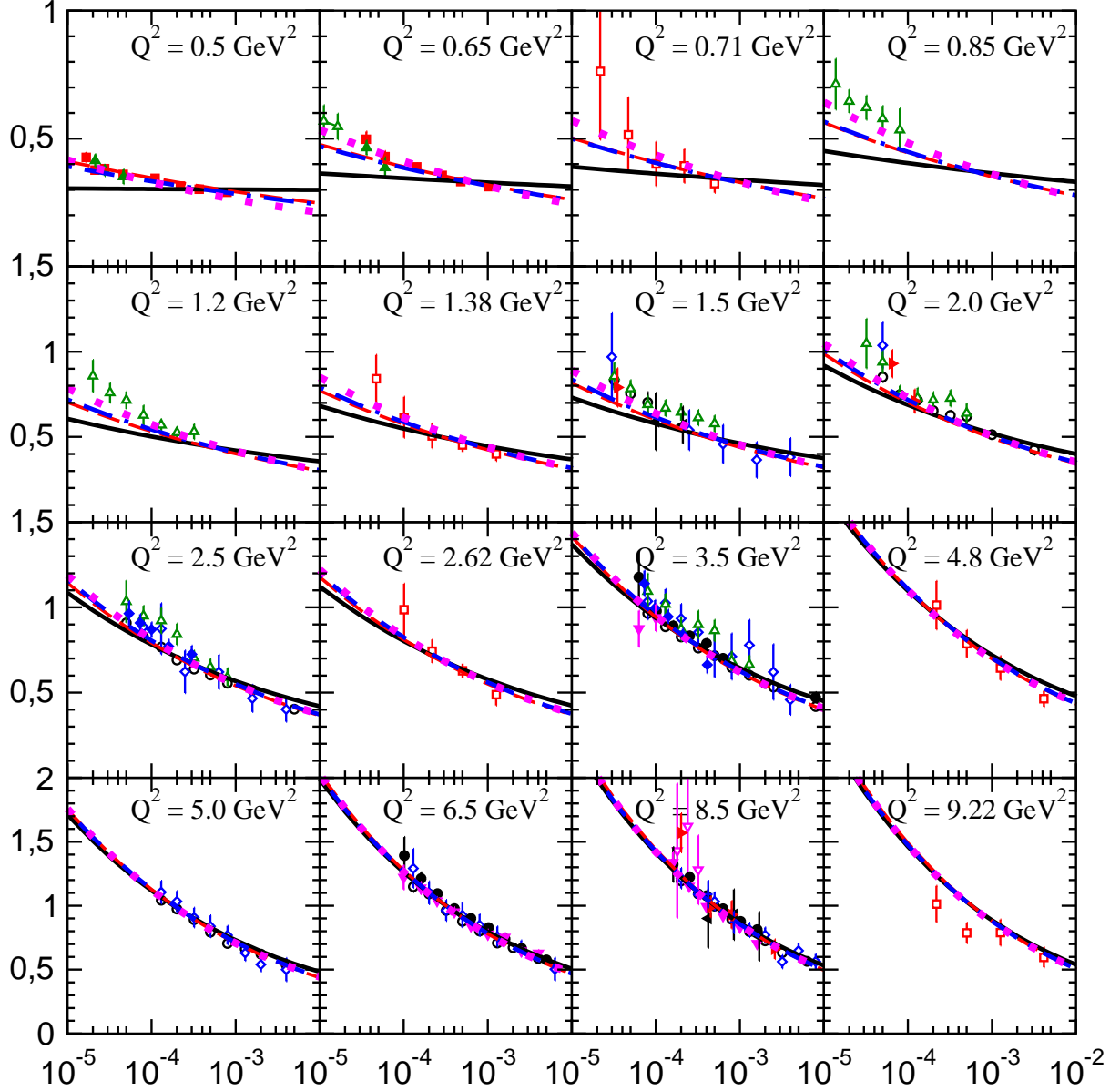


Figure 1: x dependence of $F_2(x, Q^2)$ in bins of Q^2 . The experimental data from H1 (open points) and ZEUS (solid points) are compared with the NLO fits for $Q^2 \geq 0.5 \text{ GeV}^2$ implemented with the canonical (solid lines), frozen (dot-dashed lines), and analytic (dashed lines) versions of the strong-coupling constant. For comparison, also the results obtained in Ref. [28] through a fit based on the renormalon model of higher-twist terms are shown (dotted lines).

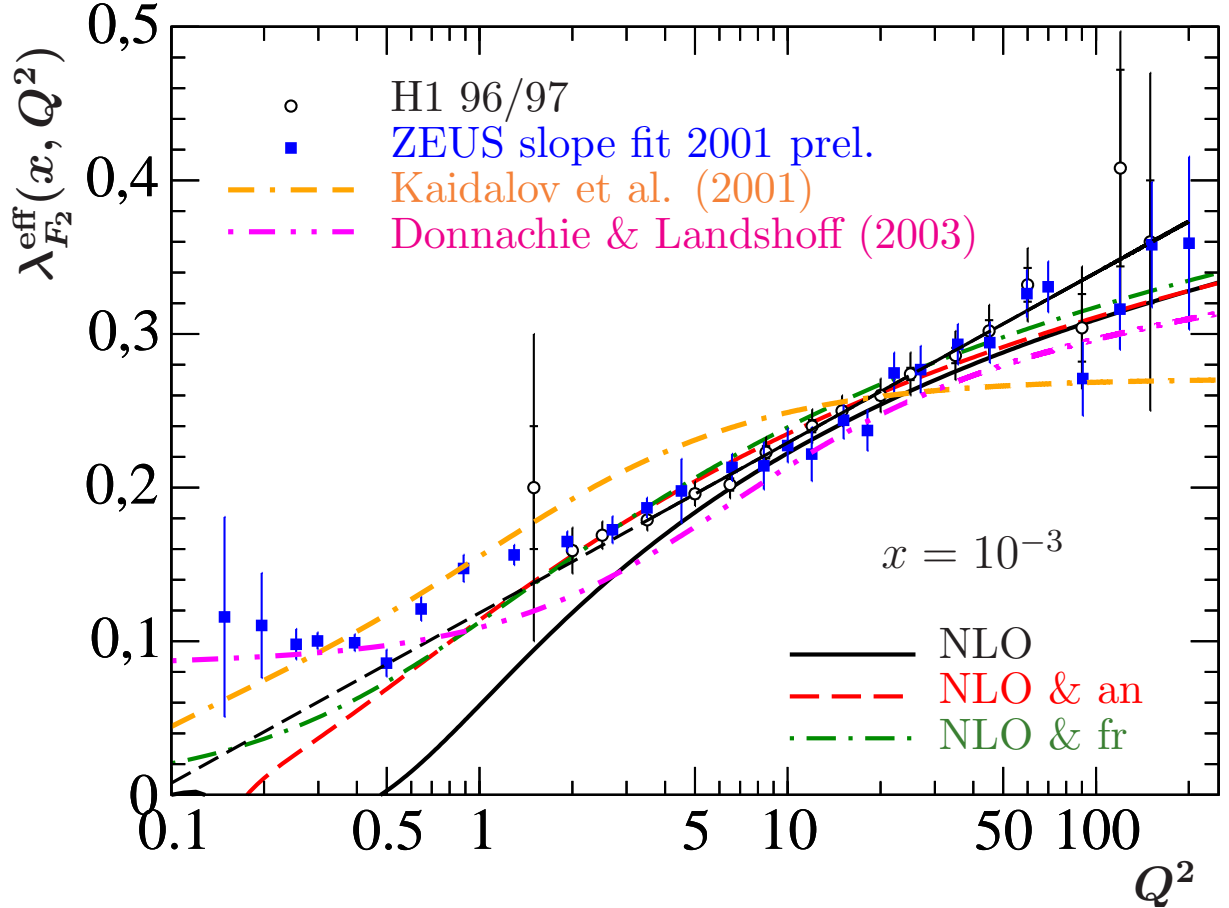


Figure 2: Q^2 dependence of $\lambda_{F_2}^{\text{eff}}(x, Q^2)$ for an average small- x value of $x = 10^{-3}$. The experimental data from H1 (open points) and ZEUS (solid points) are compared with the NLO fits for $Q^2 \geq 0.5 \text{ GeV}^2$ implemented with the canonical (solid line), frozen (dot-dashed line), and analytic (dashed line) versions of the strong-coupling constant. The linear rise of $\lambda_{F_2}^{\text{eff}}(x, Q^2)$ with $\ln Q^2$ as described by Eq. (2) is indicated by the straight dashed line. For comparison, also the results obtained in the phenomenological models by Kaidalov et al. [47] (dash-dash-dotted line) and by Donnachie and Landshoff [48] (dot-dot-dashed line) are shown.

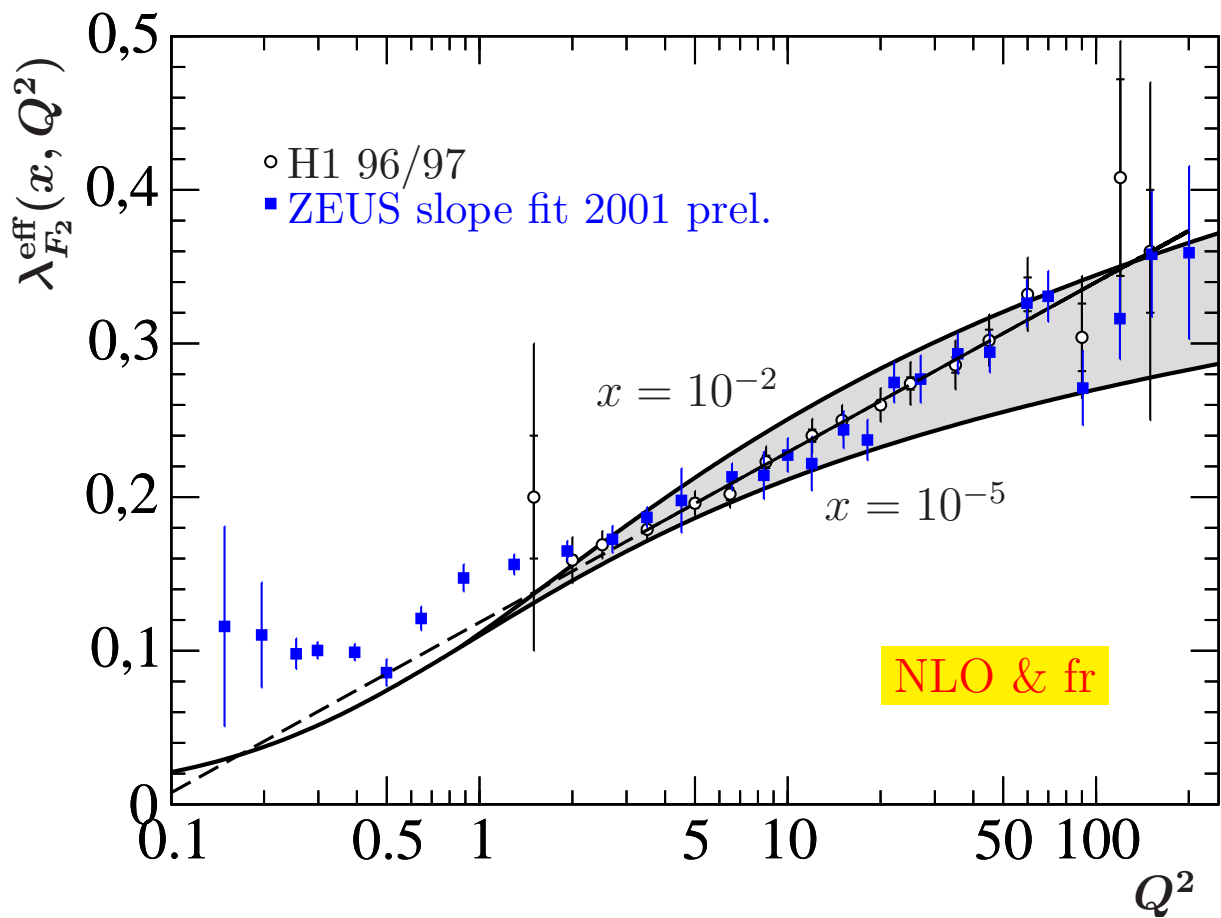


Figure 3: Same as Fig. 2, but for the NLO fit implemented with the frozen version of the strong-coupling constant and for x in the range $10^{-5} < x < 10^{-2}$.